Light-curve Recovery with Rubin-LSST. II. Unveiling the Darkness of the Galactic Bulge (VESTALE) with RR Lyrae

M. Di Criscienzo[1], S. Leccia[2], V. Braga[1], I. Musella[2], G. Bono[3], M. Dall'Ora[2], G. Fiorentino[1], M. Marconi[2], R. Molinaro[2], V. Ripepi[2], L. Girardi[4], A. Mazzi[5], G. Pastorelli[6], M. Trabucchi[6], N. Matsunaga[7], M. Monelli[8], A. Saha[9], K. A. Vivas[10], and R. Zanmar Sanchez[2]

[1] INAF—Osservatorio Astronomico di Roma, Via Frascati 33, I-00078 Monte Porzio Catone, Roma, Italy
[2] INAF-Osservatorio Astronomico di Capodimonte, Salita Moiariello 16, 80131 Naples, Italy
[3] Department of Physics, Università di Roma Tor Vergata, Via della Ricerca Scientifica 1, 00133 Roma, Italy
[4] Osservatorio Astronomico di Padova—INAF, Vicolo dell'Osservatorio 5, I-35122 Padova, Italy
[5] Università di Bologna, Italy
[6] Dipartimento di Fisica e Astronomia Galileo Galilei, Università di Padova, Vicolo dell'Osservatorio 3, I-35122 Padova, Italy
[7] Department of Astronomy, School of Science, The University of Tokyo, 7-3-1 Hongo, Bunkyo-ku, Tokyo 113-0033, Japan
[8] Instituto de Astrofísica de Canarias, Calle Via Lactea s/n, 38205 La Laguna, Tenerife, Spain
[9] National Optical Astronomy Observatory, 950 N. Cherry Avenue, Tucson, AZ 85719, USA
[10] Cerro Tololo Inter-American Observatory/NSF's NOIRLab, Casilla 603, La Serena, Chile
Received 2024 May 13; revised 2024 June 12; accepted 2024 June 12; published 2024 August 7

Abstract

This work is part of VESTALE, a project initiated within the Legacy Survey of Space and Time (LSST) Cadence Strategy Optimization Process. Its goal is to explore the potential of Rubin-LSST observations aimed at the Galactic bulge (henceforth just "Bulge") for studying RR Lyrae (RRL) stars. Observation and analysis of RRL stars in the Bulge are crucial for tracing the old population of the central part of our Galaxy and reconstructing its formation. Based on observations conducted with CTIO/DECam by Saha et al. toward Baade's window, our simulations demonstrate that early Rubin-LSST observations will enable the recovery of RRL light curves (LCs) at Galactic center distances with sufficient precision. This will allow us to utilize theoretical relations from Marconi et al. to determine their distances and/or metallicity, following the REDIME algorithm introduced in Bono et al. We show how reddening and crowding affect our simulations and highlight the importance of considering these effects when deriving pulsation parameters (luminosity amplitudes, mean magnitudes) based on the LCs, especially if the goal is to explore the opposite side of the Bulge through the observation of its RRL. The simulations discussed in this investigation were conducted to support the Survey Cadence Optimization Committee's decision to observe this important sky region since it has only recently been decided to include part of the Bulge as a target within the LSST main survey.

Unified Astronomy Thesaurus concepts: RR Lyrae variable stars (1410); Sky surveys (1464); Galactic bulge (2041); Time series analysis (1916)

1. Introduction

Although detailed photometric investigations of the Galactic bulge (henceforth just "Bulge") date back to more than a century ago thanks to the pioneering works of Shapley and Baade, its formation and evolution remain a debated topic (Kunder 2022).

Old, metal-poor stars in the inner Galaxy need to be adequately accounted for when discussing processes that gave rise to the formation of the Galactic bar/bulge. In general, RR Lyrae (RRL) can be easily recognized among these old stars, due to the coupling between the shape of the light curve (LC) and the pulsation period, and for this reason, they are often used as tracers of old stellar populations in different Galactic and extragalactic environments.

Even if the Bulge is a challenging environment owing to the effect of high reddening and stellar crowding, several studies have successfully investigated the RRL's LCs in the past decade. We can mention, for example, MACHO, EROS, and OGLE, optical surveys dedicated to microlensing, which

discovered thousands of variable stars in the Bulge (Renault et al. 1997; Alcock et al. 1998; Soszyński et al. 2019), or the VVV survey (Contreras Ramos et al. 2018), which, working in the near-infrared bands, has the advantage of being less sensitive to reddening than those in the optical passbands, and indeed, they discovered 1000 new RRL in the Galactic center.

Recent studies based on these large samples (see Kunder 2022, for a complete review) show that the Bulge RRL have a metallicity distribution function centered around [Fe/H] ~ -1.4, but covering a very broad range in iron abundance (Terndrup & Walker 1994; Savino et al. 2020). This means that RRL are solid tracers to investigate the early chemical enrichment of the Bulge (Debattista et al. 2023). As for the kinematic properties, there still needs to be a consensus as to whether the Bulge RRL spatially trace out the bar or they are more consistent with a more spheroidal Bulge population. In particular, different RRL photometric surveys in different wavelengths present differing results. To further complicate the situation, many of the results from current investigations are affected by several limitations: (i) deep and homogeneous optical investigations have been limited to low reddening windows, and (ii) the Bulge, in particular the inner part, is among the densest Galactic stellar fields. This means that both optical and near-infrared seeing-limited observations are

hampered by two limitations: (i) even relatively bright sources are affected by blending, and (ii) the limiting magnitude is quite shallow, due to the confusion limit. This paper will focus on what the soon-to-start Rubin Legacy Survey of Space and Time (Rubin-LSST) can do for the RRL observation in the Bulge. In particular, in Marconi et al. (2022) we have derived new theoretical color–color and period–luminosity–metallicity relations for RRL in the Rubin-LSST filters based on a recently computed extensive set of nonlinear convective pulsation models for RRL stars, covering a broad range of metal content. As demonstrated in Bono et al. (2019), these relationships offer an important tool for deriving the metallicity, distance, and reddening of these stars from the recovery of their LCs. However, an accurate recovery of RRL LCs is necessary to precisely determine pulsational parameters and thus fully exploit the Marconi et al. relationships. As a part of the "unVEil the darknesS of The gAlactic buLgE" (VESTALE) project (Bono et al. 2018), in this paper we will simulate Rubin-LSST observations of RRL in the Galactic center direction, to examine the level of accuracy we can expect in the recovery of LCs and to understand how deep into the darkness we can go. This provides an exceptional opportunity to determine the density profile of old stellar populations in the direction of the Bulge. We remember that this particular footprint was only recently included in the main survey as a result of the cadence strategy optimization process and in response to the pressure from the scientific community interested in this important part of the Galaxy (Street et al. 2023).

To understand how much the decisions made at the end of Phase 2 of the Cadence Strategy Optimization Process will impact the accuracy in the recovery of Bulge RRL, in this paper we will use both tools released by the LSST Collaboration and our own. The structure of the paper is as follows. In Section 2, we will review the decisions made by the Survey Cadence Optimization Committee (SCOC) that impact the Bulge, as summarized in `baseline_v3.3_10yrs.db`. In Section 3, we show the Rubin-LSST simulations of RRL LCs discovered and studied by Saha et al. (2019) with CTIO/DECam. We analyze LC recovery as a function of time to understand how much better Rubin-LSST will be able to perform and when the first useful results for studies of Bulge formation will begin to be obtained. Section 4 investigates the effect of crowding on the recovery of RRL LCs and discusses the importance of including crowding-related errors as data products in each release of Rubin-LSST data. Considering that, in addition to extending Saha's work to a much broader sky area toward the Bulge, the survey will probe much deeper than any other survey of its kind in Section 5, where we displace Saha's templates farther away and repeat the LC recovery to understand the extent of LSST's capabilities. Conclusions are given in Section 6.

2. The Inner Part of the Galactic Bulge in Rubin-LSST OpSim Simulations

The first released simulations produced by the Operations Simulator (OpSim) within the Metrics Analysis Framework (MAF) omitted the consideration of the Galactic bulge/inner disk (and the Magellanic Clouds) in the primary survey, due to issues related to crowding. Instead, these specific sky regions were encompassed by a series of ad hoc minisurveys, each

comprising approximately one-fourth the number of visits projected by the main survey.

Thanks to the pressure of the scientific community (see, e.g., Olsen et al. 2018), the SCOC in its final document (Phase 2 document, PSTN-055[11]) added the suggestion to include part of the Galactic bulge and plane in the main survey, called the Wide–Fast–Deep (WFD) survey. In particular, the recommended footprint implemented in the last version of the baseline (`baseline_v3.0_10yrs.db`) included a ∼10% area increase, extending the WFD into low-dust extinction regions for extragalactic science, and expanded WFD-level coverage into high-priority regions for Galactic science: the Bulge and the Magellanic Clouds. The proposed solution is to cover the Galactic plane in two parts: WFD-level regions near the Bulge and other regions of interest (which are still to be decided in a definitive manner), and a lower level of coverage in the rest of the regions. The median number of visits per pointing in these areas over the lifetime of the survey (in any filter) is ∼800 in WFD-level areas and ∼250 in the high dust extinction (low-coverage) Galactic plane regions. Actually, there is still a preference for a distribution of visits in the *rizy* bands (20% in each of these bands), while ∼7% and 10% of the visits will be in the *u* and *g* bands, respectively.

Nevertheless, a few outstanding points remain open for further exploration and refinement. A new task force that formed immediately after the conclusion of Phase 2 of the Cadence Strategy Optimization process is currently working to provide input on the final design of the coverage of areas of the Galactic plane/bulge. In particular, the 4th Survey Cadence Optimization Workshop[12] has just concluded and one of the requests from the SCOC at the meeting was to provide feedback on the latest simulations, especially from the Stars, Milky Way, and Local Volume Science Collaboration. This group is particularly interested in using LSST data to reconstruct the shape and evolution of the Galaxy and its components. This work partially aims to address this request.

In addition, this exploration provides us with the opportunity to explore, for the first time, the new simulations constructed considering the triple silver coating of the telescope's mirrors. We recall that the sensitivity has notably improved in *grizy* photometric bands between baseline version 3.0 (described in the Phase 2 document) and version 3.3 and decreased by approximately 0.4 mag the *u*-band sensitivity.

3. LSST Recovery of RR Lyrae Observed by Saha et al. (2019) in Baade's Window

To simulate LSST observations of RRL in the central part of the Galaxy, we use the PulsationalStarRecovery (PSR) tool that we built within the Cadence Survey Optimization process to analyze the recovery of the LSST simulated LCs (Di Crisciozo et al. 2023).

We start from the area centered on the well-known Baade's window ((*l*, *b*) = (1.02, −3.92) deg), which has the advantage of being close to the direction of the Galactic center while remaining relatively transparent to dust. The further advantage of this area is that *ugriz* observations at different epochs with the DECam imager on the Blanco 4 m telescope at CTIO are available. DECam has not only similar filters but also a pixel scale very similar to LSSTCam. Saha et al. (2019) observed a
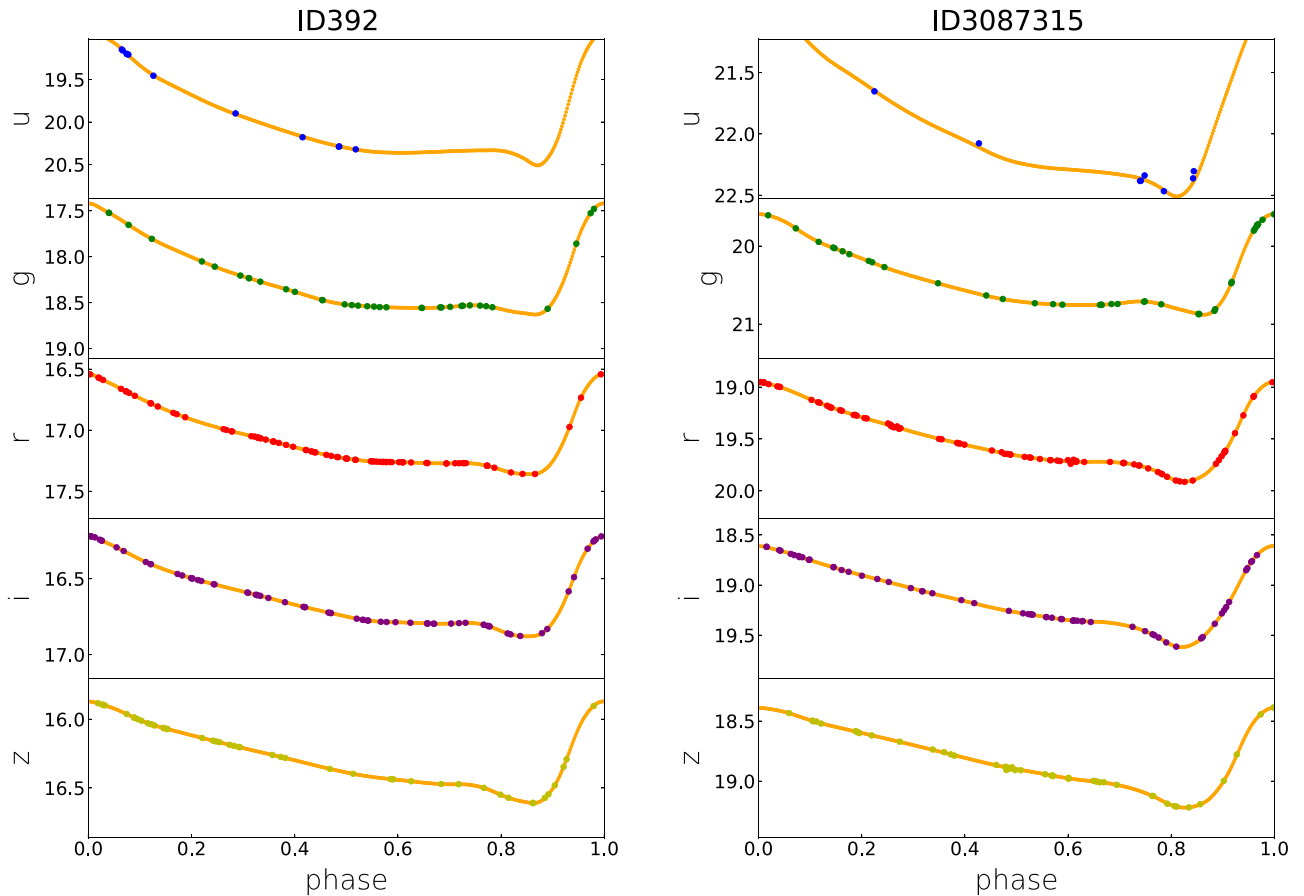

Figure 1. Simulated LSST observations during the first 4 yr in *ugriz* colors (colored points) for two RRL in Saha's sample. Star 3087315 is the faintest in their sample. The orange LC is Saha's template. Photometric errors (<0.001 mag) derived from OpSim and used in this simulation are too small to be shown.

single DECam field (field of view $= 3$ deg^2) in Baade's window, obtaining between 70 and 90 epochs per band. According to the last OpSim version (`baseline_-v3.3_10yrs.db`), the Baade's window region will be observed by the main survey, which means that it will receive an average of 800 visits over the 10 yr of the survey in all the photometric bands.

Using these data, Saha et al. (2019) confirmed and analyzed almost 500 RRL, almost all ab-type. For each of the confirmed RRL the authors provided the best template taken from the library of LC templates (LCTs) set up from Sesar et al. (2010). We use those curves as starting points to derive the simulated LSST LC.

From Saha's sample we only removed stars that have, in at least one photometric band, an average magnitude brighter than the saturation magnitude of Rubin-LSST (see the LSST Science Book at https://www.lsst.org/scientists/scibook). As a result, the number of RRL that we simulated decreased from 474 to 439 stars.

We begin analyzing the recovery of RRL as they would appear if the LSST cadence followed one of the latest baselines released by SCOC (namely `baseline_v3.3_10yrs.db`).

In Figure 1, we exhibit two of the simulated time series obtained in all available filters after 4 yr of LSST observations, phase-aligned using the periods derived by Saha (orange curve). It should be noted that unfortunately the Saha observations are missing the *Y* band, and for this reason, we did not simulate the observations in the Rubin-LSST *y* band. The star ID3087315 is the faintest among Saha's that,

nevertheless, falls within Rubin detection capabilities (single-visit 5σ mag are 23.3, 24.4, 23.8, 23.6, and 22.9 in *u*, *g*, *r*, *i*, *z* filters, respectively). We have started by selecting the visits predicted for the first 4 yr of the survey because, according to the simulated LSST observational strategy, it is after this duration that, on average, the total number of visits will be comparable to those obtained by Saha ($\sim$250/300 phase points if all the bands are considered and $\sim$60/70 in the "*i*" band). Coincidentally, this is also the average number of visits expected for the low coverage of the Galactic plane regions (see Section 3.1). In the top panel of Figure 2, we present the comparison between the periods derived by the PSR metric on 4 yr LSST simulated time series and Saha's periods. Note that our tool uses Gatspy software (VanderPlas & Ivezic 2015) to derive periods. In particular, we use the MultibandLombScar-gle option that performs a Lomb–Scargle (Lomb 1976; Scargle 1982) period search, by using simultaneously the information from all the available filters. After 4 yr, we found that the period is recovered excellently: within 0.005% for all the stars and within 0.001% for more than 50% of the star's sample. The middle and bottom panels of Figure 2 display the trend with the template's mean magnitude of the difference between the recovered and template mean magnitudes (in *r* band) after the phased LC was fitted by our metric. The PSR metric's version used in this work differs from the one published in Di Criscienzo et al. (2023), as it autonomously computes the required numbers of harmonics, thus reducing the degrees of freedom in the fit. Our analysis demonstrates that in the WFD survey after 4 yr LSST will recover Saha's LCs with such
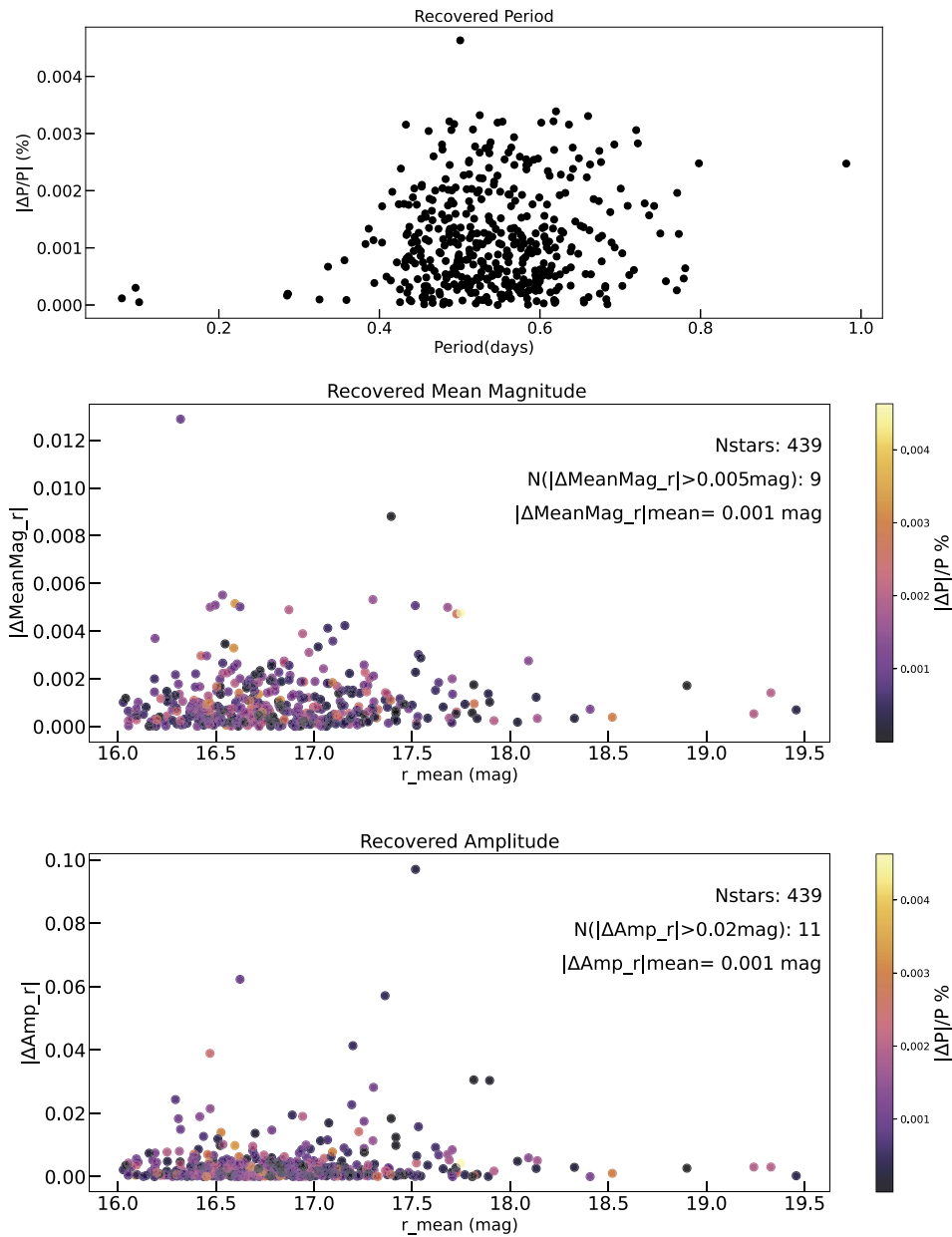
Figure 2. Relative difference (in percentage) between recovered and template periods (top), mean magnitude (middle), and amplitude (bottom) as a function of *r* mean brightness for the 439 RRL from Saha's sample. In the middle and top panels the vertical bar reports the accuracy of the recovery of the period.

precision that it provides very accurate mean magnitudes and peak-to-peak amplitudes (∼0.001 mag). It is crucial to note that these quantities, especially periods and mean magnitudes, go in the period–luminosity relations that are used to determine distance and/or metallicity. Thus, the high precision of the recovered parameters also implies extremely reliable distance and metallicity determinations. Instead, amplitude is less important for distances, but it is relevant to study the properties of the RRL population through, for example, a Bailey diagram (Fiorentino et al. 2015, 2022).

The only error we have considered at this stage on the individual visit magnitude is the photometric error derived from the 5σ limiting magnitude given by OpSim at each position in the sky, which, notably, for the magnitudes involved, is exceedingly small (less than 0.006/0.007 mag in all the photometric bands). This factor also explains why our LC exhibits much less dispersion around the template

compared to Saha's LC, which exhibits a 0.03/0.04 mag mean scatter around the template in the *griz* photometric bands and up to 0.09 mag in the *u* band (see their Figure 1).

We did not take into consideration the crowding effect on the template, assuming that Saha et al. (2019) accurately deblended their stars during their photometry. The effect of the crowding will be discussed in detail in Section 4.

3.1. Early Science: Unveiling Key Insights from the Very First Releases

To investigate the LSST recovery of RRL LCs from the very first release, in Figure 3 we show the differences between recovered and true periods/mean magnitudes after 1, 2, 3, and 4 yr.

Despite the first data release being expected 6 months after the survey's start, we did not consider this release in the figure
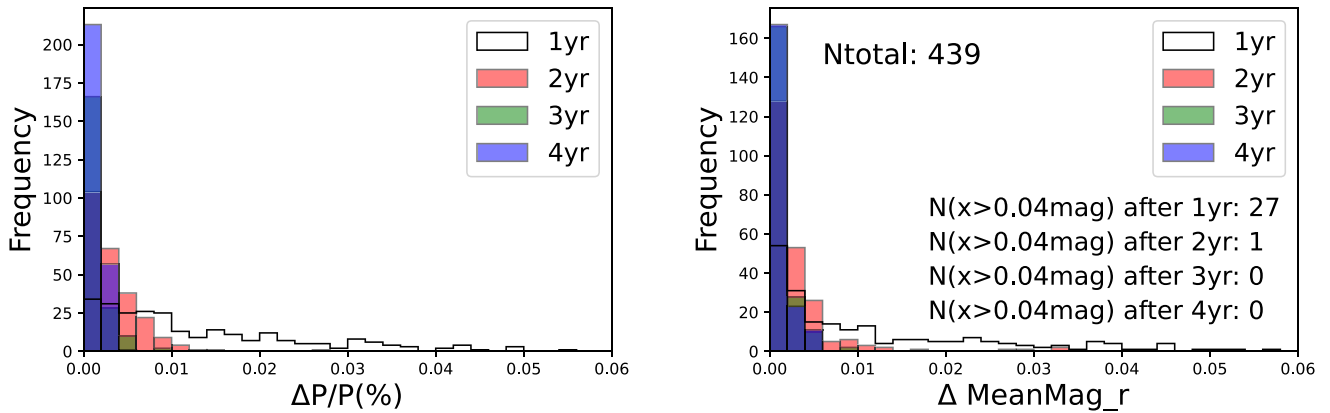
Figure 3. Precision distribution in the recovery of period and average magnitude of RRL in the Saha sample after 1, 2, 3, and 4 yr. The analysis of the right panel shows that, starting from the second year, the precision in the *r* band remains below 0.04 mag.

because in that case the number of visits strongly depends on the type of rolling conducted during the first part of the year—a matter that, even though fundamental in defining LSST's early science and extensively discussed in the Phase 2 document, falls beyond the scope of this work.

As expected, our simulations show that the accuracy in recovering the LC increases with the number of visits, but it is enough for doing early science even after 1 yr. Entering in more detail, we will recover periods with a precision smaller than 0.005% for almost half of the sample, while, in general, they will all remain below 0.05% (which translates to about 4 s for a typical RRL) from the first year.

Figure 3 also shows that, from the first year, *r*-average magnitudes will be recovered within 0.04 mag. Instead, the same precision in the *g* band will be achieved by more than 90% of the stars in the Saha sample only starting from the second year, while the number of visits in the *u* band is too small (<7 phase points) to allow a good fit of the data.

Starting from the very first release, LCTs can be adopted in this case to estimate accurate mean magnitudes (V. Braga et al. 2024, in preparation). LCTs can be used either by anchoring them on a single phase point (but this requires the knowledge of the reference epoch) or as fitting functions, for which at least three/four-phase points are needed, but only the pulsation period is required. This tool will be mostly useful during the first 2 yr of the survey—when a precise fitting of the LC will not be possible, due to the small number of phase points—thus allowing the exploitation of the early scientific data from LSST. In conclusion, with Rubin-LSST we will obtain LCs at least as accurate as those derived by Saha et al. (2019) from the early years of the Rubin-LSST survey and, additionally, over a wider and deeper footprint with the large advantage of exploring a much larger portion of the Bulge. For example, setting the threshold at 0.04 mag on the mean magnitude, which is the constraint imposed by Bono et al. (2019) for the use of the REDIME method to simultaneously measure individual distances, reddening, and metallicities of RRL, our simulations show that these are achieved from the first year in the *riz* (and *y*) and from the second year in the *g* band. The visits in the *u* band within the first 4 yr, however, are too few to allow for an adequate fit, and in that case the use of templates will be necessary.

The analysis just described is also useful for understanding the problems related to the recovery of RRL's LCs located in the inner disk region, which will be observed by LSST only in

a low-density mode according to the last OpSim. Specifically, in 10 yr of LSST, this region will receive only 250 visits, coincidentally the same number of visits after 4 yr of the WFD survey. If the filter balance remains the same as in the WFD survey, in the inner/bulge areas of the Galaxy observed with a low-density cadence we can expect that observations in the *u* band for fitting the LC will be practically useless even after 10 yr. This makes it necessary to use templates in the *u* band throughout the entire duration of the survey.

4. Crowding Effect on Light Curves

So far, we have used Saha's templates from Sesar et al. (2010) and analyzed their recovery without considering the effect caused by crowding.

Extending the analysis beyond the Baade's window region and going deeper than Saha's variables, which are the two main advantages of Rubin-LSST, also means having to tackle complicated issues such as crowding and reddening. In the upcoming sections, we will address these previously over-looked questions.

It is well known that photometry in a crowded field could lead to inaccurate measurement of the flux at each visit. In general, if the star is not well deblended from the neighboring stars, at each visit the measured flux will also include the flux from the surrounding stars. Naturally, this effect depends on both the density of stars in the field under consideration and the types (luminosity and color) of the blending stars. To show the impact of crowding on the recovery of LCs during LSST, we used a TRILEGAL simulation of the Galaxy described by Dal Tio et al. (2022) that is made available at the NOIRLab Astro Data Lab (Olsen et al. 2018).

In Figure 4, for example, we show the LC of one of our sample's templates, together with that obtained adding to each visit the flux of the stars falling within a radius equal to the LSST pixel scale. In particular, for the RRL shown in this figure (ID392) TRILEGAL finds five very faint stars with *r*-band magnitudes ranging from 21.35 to 26.68 mag. In the worst-case scenario,[13] where the brightness of nearby stars is detected as the brightness of the RRL, the effect would be to have LCs brighter by approximately 0.04 mag in *r* band (see Figure 4). Another important effect is that the crowding

---

[13] Albeit unlikely because any photometry software would recognize these blending stars.
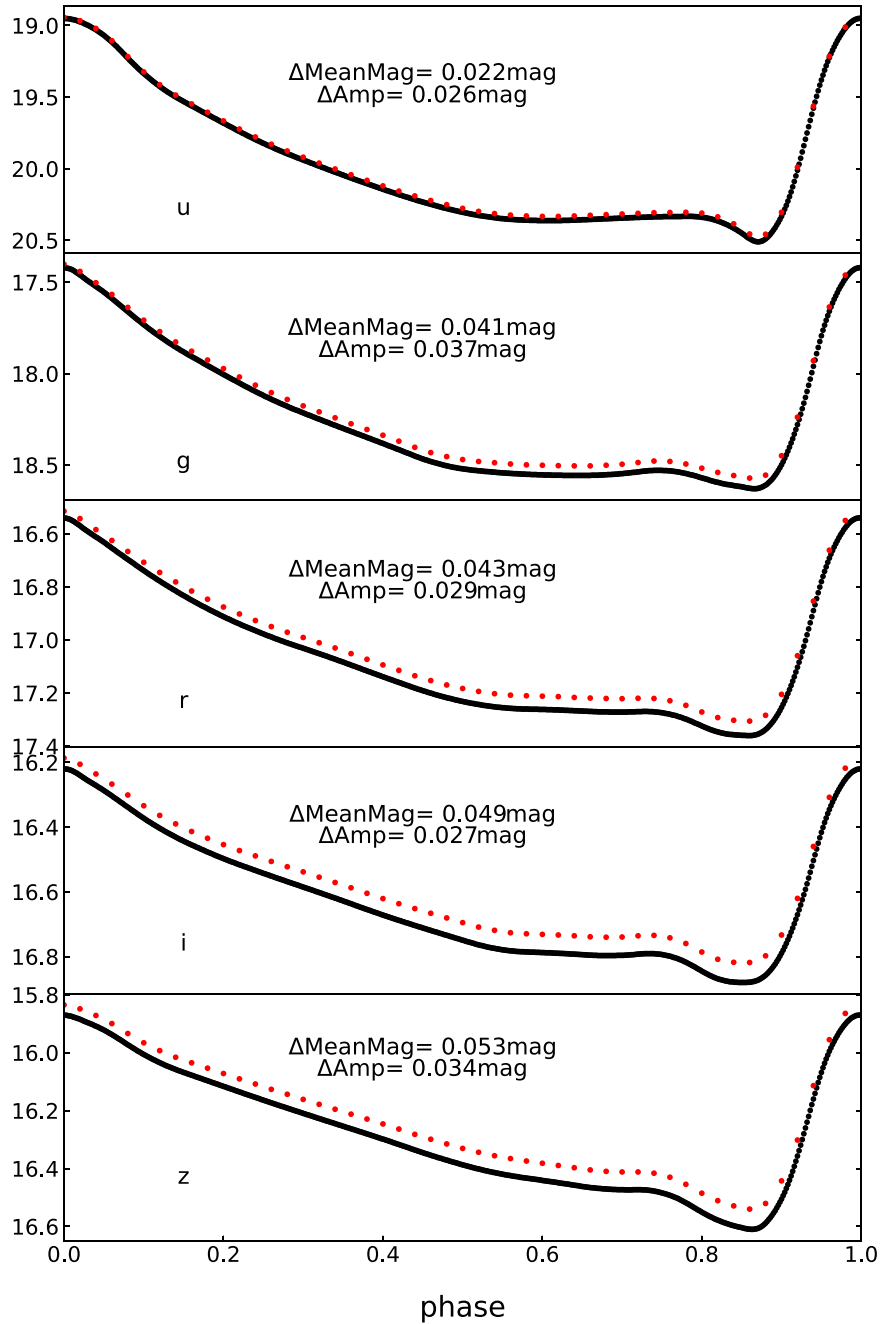
Figure 4. Comparison in *ugriz* bands between Saha's LC corresponding to the RRL star ID392 and the one obtained by adding the flux of five nearby stars according to TRILEGAL (see text). The difference between the average magnitudes and the amplitudes is reported in each panel.

decreases the RRL amplitude, due to its greater fractional contribution at minimum versus maximum light.

By doing the same exercise for all the other stars in Saha's sample, which, being in different positions, have different blending stars, the differences between recovered and template mean magnitudes remain for the investigated bands of the same order of magnitude, although they can reach up to one-tenth of a magnitude in cases where blending stars are very luminous.

Obviously, providing a precise measure of the error due to crowding is a much more complex operation that requires artificial-star tests, where fake stars are added to the observed images and then recovered using the same pipeline used for the original images. Fortunately, approximate methods exist for determining the error function from simulations. One of these

methods is described by Olsen et al. (2003) and suggests that the photometric errors due to stellar crowding, σ_{crowd}, depend on an integral of the brightness distribution of stars fainter than the faintest one being observed. This method is actually used in the MAF metric `CrowdingMagUncertMetric` developed by some coauthors of this work and described in Dal Tio et al. (2022). In Figure 5, we present the values obtained with this metric taking into account positions and magnitudes (in the labeled bands) for the objects in Saha's sample. It is noteworthy not only that these errors are of the same order of magnitude as the scatter observed in Saha's LC but also that they are larger than the precision on the average magnitudes we obtained from the recovery of the simulated LC. These computed crowding errors should be considered as errors on
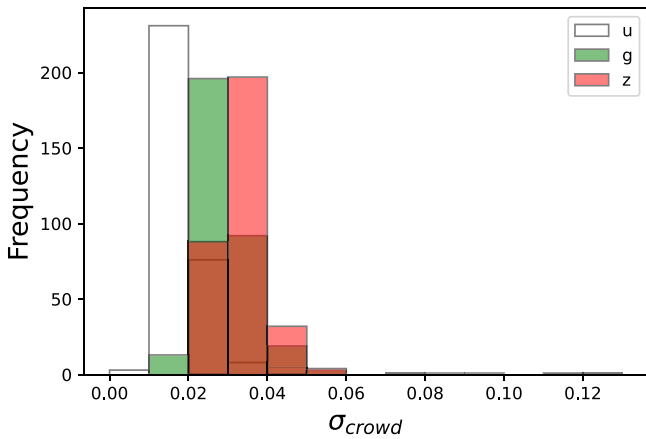
Figure 5. Histogram of photometric errors σ_{crowd} due to stellar crowding derived using `CrowdingMagUncertMetric.py` for the RRL of the Saha sample in the labeled band.

the zero-point of the recovered LC (in the brighter direction). Therefore, these errors should be associated with the mean magnitude obtained from the LC fitting together with ΔMeanMag derived by the PSR metric.

LSST Data Release is not planning to include estimates of incompleteness and photometric errors due to crowding (see the LSST Data Products Definition Document at https://lse-163.lsst.io/). As demonstrated in this section, these estimates are essential to understand the uncertainty obtained in the recovery of LCs of pulsating stars, but more generally these estimates are necessary to transform star counts into absolute quantities such as stellar volume densities and lifetimes in different phases of the stellar evolution and to be able to fit the physical models to the stellar data. For this reason, we strongly suggest that crowding errors be considered a significant added value to be associated with LSST Data Releases.

5. Probing the Far Side of the Bulge with LSST

So far, we have explored how Rubin-LSST will be able to recover Saha's RRL LCs over time and the level of precision that will be achieved with each release, aware that the advantage of Rubin-LSST will be that of extending Saha's work to a much larger portion of the sky than that observed by DECam. In this section, instead, we investigate to which photometric depth can RRL be observed/recovered. This is crucial information for understanding our ability to reconstruct the geometry and formation history of the Bulge using LSST data.

To this purpose, we take star ID392, which, according to Saha's computations, is located at $d_{\mathrm{saha}} = 9.09\,\mathrm{kpc}$ and has a color excess $E(r-z) = 0.86\,\mathrm{mag}$, and while staying within Baade's window, we move the star away using different ratios of d_{saha}, which thus becomes our distance unit. To account for the increase in reddening, an additional color excess had to be added to each new distance to derive the simulated LC. This additional color excess takes into account the high probability of encountering a significant amount of dust on the other side of the Bulge. Specifically, for all the distances larger than d_{saha} we assumed that the additional excess is equal to the quantity calculated by Saha using the minimum LC method (Sturch 1966) on our side. This assumption is based on the spherical symmetry of the dust around the Galactic center, with a drop to zero when radius $R = d_{\mathrm{saha}}$. We acknowledge that this is only

an approximation, but without access to models of dust distribution beyond the Galactic center,[14] it is the only plausible approach.

Actually, the awareness of this uncertainty makes still more evident the importance of multiwavelength LSST observations of RRL stars toward the Bulge and will help to derive reddening maps, either using the appropriate combination of theoretical relations from Marconi et al. (2022), as suggested by the REDIME method (Bono et al. 2019), or directly from RRL LCs, as done by Saha et al. (2019), using the color at minimum light of the RRL. Figure 6 separately shows, for each band, the ratio between the limiting magnitude (derived from OpSim) and the ID392's mean magnitude as the distance of the star increases. Obviously, due to the increased reddening in the u band,[15] this limit in the bluest available photometric band is reached at shorter distances with respect to the others. In particular, for the considered extra reddening in the specific case, doubling the distance already brings the magnitudes below the photometric threshold. For the other bands, however, the figure shows that in principle it is possible to observe stars up to four times the original distance, up to just under $\sim$40 kpc. However, at these distances, the so-called crowding limit (the brightness below which the incompleteness caused by crowding becomes significant, assuming values above approximately 50%) is reached. As reported by Dal Tio et al. (2022), this closely corresponds to the point where the near-infrared magnitude will first reach $\sigma_{\mathrm{crowd}} \sim 0.25$ mag. This limit also depends on the instantaneous value of the seeing; in particular, for the case in question, we used the minimum seeing in the first 4 yr of simulations ($0''51$), and for this reason, the values plotted in the figure represent a lower limit. This is true especially for the near-infrared bands riz (and y when it will be available), while in the case of the g band this limit is reached before, and in particular at three times the distance of Saha.

For all distances between the true distance of the template and the limit distance due to the crowding, LSST provides valuable data for discovering new RRL stars. The time series of these newly discovered variables will allow us to achieve excellent accuracy on the period (up to $\Delta P = 10^{-6}$ days). We are also able to reconstruct the shape of the LC and hence to derive its zero-point representing the mean magnitude. But for the errors on this value, as stressed in the previous section, we cannot consider only those coming from the fitting procedure, but we have to take into account the larger uncertainties due to the effect of crowding on the zero-point of the LC. In our test case, for example, σ_{crowd} ranges from 0.2 mag in the g band to 0.1 mag in the z band aiming to make the mean magnitudes brighter. If these errors are not properly taken into account, we would derive, on average, smaller distances of those RRL observed on the opposite side of the Bulge that are brighter than the crowding limit, leading to an incorrect reconstruction of the shape of the inner part of the Milky Way. Unfortunately, even at 1.5 times the distance of Saha ($\sim$13.5 kpc), the errors are still significant even if they drop below 0.1 mag in our reddest band z, and they presumably remain equally small even in the y band, which we are currently not simulating because we lack the corresponding Saha template. Therefore, we

---

[14] For example, we verified that the 3D dust Bayestar maps (Green et al. 2018) saturate at distances greater than the Galactic center in the direction of ID392.
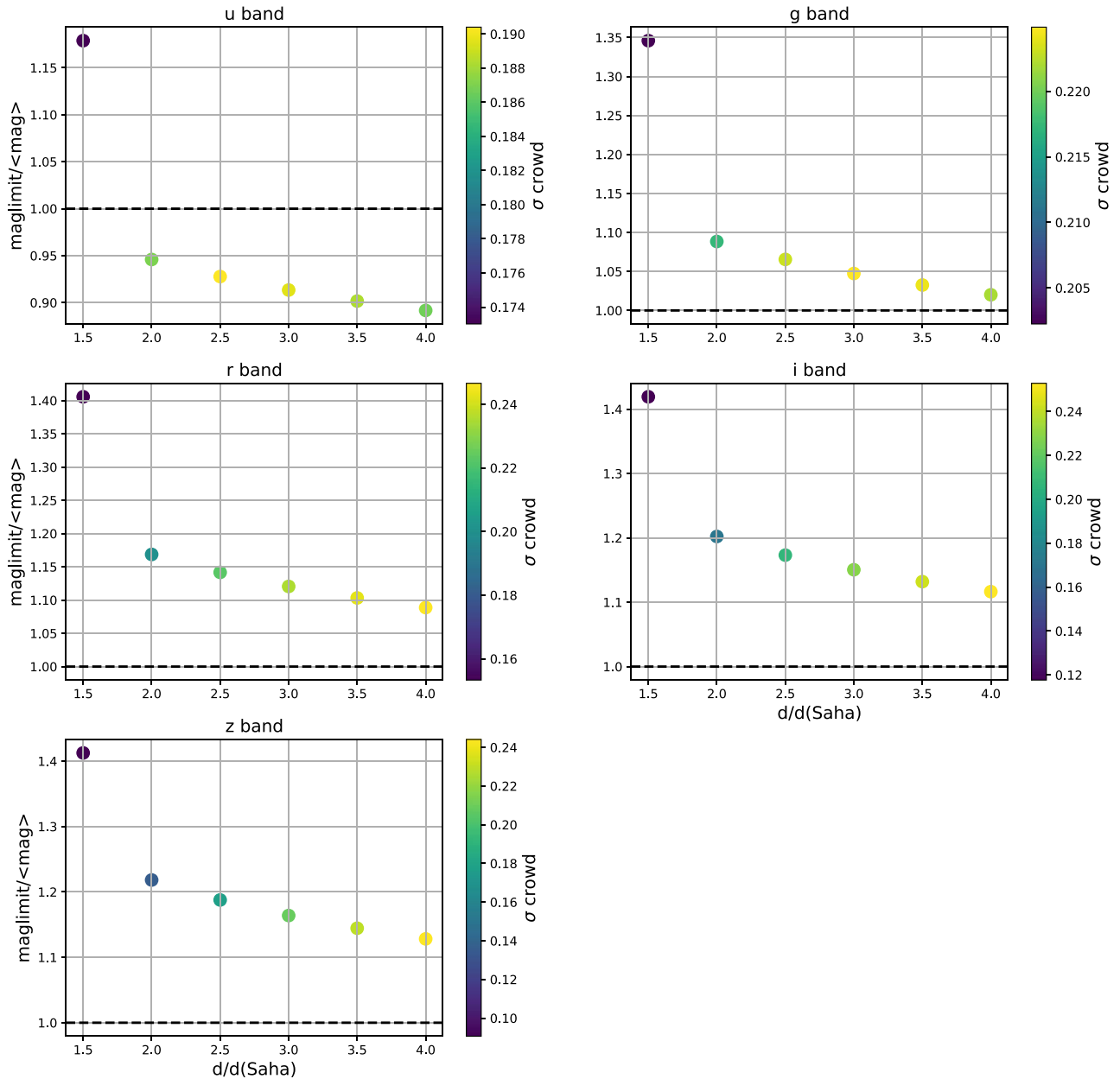[15] In particular, we adopt the $A_X/E(rz)$ ratios as given in Equations (22)–(26) of Saha et al. (2019).

Figure 6. Distance of the template's average magnitude from the limiting magnitude derived from OpSim for different template distances expressed as factors between new distance and original distance derived from Saha color coded by the σ_{crowd} value. The points below the horizontal line are unlikely to be observed by LSST according to the most recent simulations.

confirm that these two bands will be crucial for the first kiloparsec beyond the the Galactic center to characterize their LC and derive RRL pulsation parameters such as periods and mean magnitudes. Unfortunately, having mean magnitudes in only two bands means that it would not be possible to use the REDIMI method to simultaneously derive distance, metallicity, and reddening. Different methods based on the shape of the LC, such as $\phi31$–[Fe/H] relations, could be used in these cases (V. Ripepi et al., in preparation).

6. Conclusions

In Di Criscienzo et al. (2023), we employed the tool `PulsationalStarRecovery` developed by our team during the Survey Strategy Optimization process to simulate Rubin-LSST observations of RRL in selected Local Group

dwarf galaxies and quantified the recovery of their LC. We found that the observing cadence will not have a major impact on the detection and characterization of individual RRL; however, it will affect the number of RRL measured with the required photometric accuracy for properly utilizing Marconi et al. (2022) relations to derive their distances and metallicities from observational quantities such as period and mean magnitudes.

In this paper, our focus shifted toward a significantly more complex footprint: the Bulge, which was only recently included in the Rubin-LSST main survey and for which there are still many uncertainties regarding both the choice of the exact size of the footprint and the observational strategy to be used.

In this work, we have shown that high reddening and crowding of this part of the sky will affect photometric measurements during each survey visit and pose challenges to

the recovery of pulsating stars' LCs, significantly increasing the error budget on pulsation parameters, especially on average magnitudes and amplitudes.

The same considerations can obviously be extended to observations of other crowded fields, such as globular clusters or the central parts of dwarf galaxies studied in Di Criscienzo et al. (2023).

As a reference point for this work, we relied on Saha's observations with CTIO/DECam toward the Bulge. In Saha et al. (2019) the authors used these observations to reconstruct the spatial distribution of the RRL population around the Galactic center and at the same time derived detailed reddening maps. Furthermore, these observations can be combined with the Marconi et al. (2022) relations to determine the metallicity distribution of observed RRL using the REDIME method by Bono et al. (2019) or reddening maps based on the color at minimum light of RRL. Currently this is possible only in a limited small areas toward the Bulge, whereas Rubin-LSST will give the opportunity to perform similar analysis over a much broader and deeper area, providing homogeneous material for future studies of the Bulge structure, the first step in reconstructing its formation history.

In particular, our simulations show that although it will be necessary to use variable templates to accurately derive observables such as mean magnitude and amplitude, especially in undersampled photometric bands like u and g during the very early releases, using the period derived from the most sampled bands, on the contrary for the redder bands starting from DR1 the precision achieved in the LC recovery will be much higher than that obtained by Saha and collaborators. Instead, in the case of Galactic bulge/disk regions covered by the WFD survey we will have to wait for the data release at the end of the second year to achieve the same precision even in the u and g bands without using templates and even the end of the survey in the case of areas not included in the main survey.

Using TRILEGAL's simulated Milky Way by Dal Tio et al. (2022), we have analyzed the effect of crowding on the recovery of RRL LCs, emphasizing that, if not appropriately treated, we recover LCs that are brighter and with smaller amplitude. In particular, the need for a measure of crowding error starting from the early releases has been emphasized, in order to properly utilize the provided magnitudes appropriately.

We finally explored the possibilities of observing RRL stars on the opposite side of the Bulge with respect to the Galactic center. Obviously, the results depend heavily on the reddening model adopted for the dark side of the Bulge. Specifically, by making the very approximate assumption of a uniform radial distribution that decreases to zero after a radius $R = d_{saha}$, we have demonstrated that (1) observations in the u band fall below the photometric limit even before reaching $R = 2d_{saha}$, and therefore before reaching virtually the point symmetrically opposite to us; and (2) in the infrared photometric bands, the crowding limit is reached before the photometric limit, and this occurs at around 4 times the distance of the test star we used. In this case, the recovery of LCs, although it will provide very precise periods and equally good LC shapes, will give average magnitudes that will be heavily influenced by the crowding limits (between 0.1 and 0.2 mag).

Among the investigated bands, the only one to obtain distance estimates accurate enough to investigate the shape and fine structure of the bulge/bar regions well beyond the Galactic center is the z band. Additionally, we note that the y band will play a

crucial role in early science, especially in crowded and reddened regions like the inner Bulge. However, constraining the photometric accuracy in this band requires further refinement.

In general, early Rubin-LSST observations will be able to trace the edge between the Galactic bulge/bar and the thin disk, which is a very promising indication. In a recent investigation by our group (D'Orazi et al. 2024), a significant sample of field RRL with disk kinematics was identified. Despite their similarity to typical thin-disk stars, these objects exhibit systematic underabundance in α- and neutron capture elements compared to typical thin-disk stars. Once confirmed, if these findings hold true, they could pave the way for a new approach to constrain the early formation of the Galactic spheroid, particularly the early coupling between the Galactic bulge/bar and the thin disk, using the same stellar tracer. In conclusion, we strongly support the inclusion of Galactic bulge/inner disk observations in the WFD survey because LSST observations of this part of the sky, despite the limitations discussed in this paper, will be crucial for reconstructing the oldest component of the inner part of Milky way, thanks to the RRL stars that will be discovered and analyzed during the survey.

ORCID iDs

M. Di Criscienzo ● https://orcid.org/0000-0003-4132-1209
V. Braga ● https://orcid.org/0000-0001-7511-2830
I. Musella ● https://orcid.org/0000-0001-5909-6615
G. Bono ● https://orcid.org/0000-0002-4896-8841
G. Fiorentino ● https://orcid.org/0000-0003-0376-6928
M. Marconi ● https://orcid.org/0000-0002-1330-2927
R. Molinaro ● https://orcid.org/0000-0003-3055-6002
L. Girardi ● https://orcid.org/0000-0002-6301-3269
A. Mazzi ● https://orcid.org/0000-0002-7503-5078
M. Trabucchi ● https://orcid.org/0000-0002-1429-2388
K. A. Vivas ● https://orcid.org/0000-0003-4341-6172

References

Alcock, C., Allsman, R. A., Alves, D. R., et al. 1998, ApJ, 492, 190
Bono, G., Dall'Ora, M., Fabrizio, et al. 2018, unVEil the darknesS of The gAlactic buLgE (VESTALE), LSST White Paper 2018, https://docushare.lsstcorp.org/docushare/dsweb/Get/Document-30571/dalla_ora_vestale_gp.pdf

Bono, G., Iannicola, G., Braga, V. F., et al. 2019, ApJ, 870, 115
Contreras Ramos, R., Minniti, D., Gran, F., et al. 2018, ApJ, 863, 79
Dal Tio, P., Pastorelli, G., Mazzi, A., et al. 2022, ApJS, 262, 22
Debattista, V. P., Liddicott, D. J., Gonzalez, O. A., et al. 2023, ApJ, 946, 118
Di Criscienzo, M., Leccia, S., Braga, V., et al. 2023, ApJS, 265, 41
D'Orazi, V., Storm, N., Casey, A. R., et al. 2024, MNRAS, 531, 137
Fiorentino, G., Bono, G., Braga, V. F., et al. 2022, MmSAI, 93, 47
Fiorentino, G., Bono, G., Monelli, M., et al. 2015, ApJL, 798, L12
Green, G. M., Schlafly, E. F., Finkbeiner, D., et al. 2018, MNRAS, 478, 651
Kunder, A. 2022, Univ, 8, 206
Lomb, N. R. 1976, Ap&SS, 39, 447
Marconi, M., Molinaro, R., Dallra, M., et al. 2022, ApJ, 934, 29

Olsen, K., Di Criscienzo, M., Jones, R. L., et al. 2018, arXiv:1812.02204
Olsen, K. A. G., Blum, R. D., & Rigaut, F. 2003, AJ, 126, 452
Renault, C., Afonso, C., Aubourg, E., et al. 1997, A&A, 324, L69
Saha, A., Vivas, A. K., Olszewski, E. W, et al. 2019, ApJ, 874, 30
Savino, A., Koch, A., Prudil, Z., et al. 2020, A&A, 641, A96
Scargle, J. D. 1982, ApJ, 263, 835
Sesar, B., Ivezić, Ž., Grammer, S. H., et al. 2010, ApJ, 708, 717
Soszyński, I., Udalski, A., Wrona, M., et al. 2019, AcA, 69, 321
Street, R. A., Li, X., Khakpash, S., et al. 2023, ApJS, 267, 15
Sturch, C. 1966, ApJ, 143, 774
Terndrup, D. M., & Walker, A. R. 1994, AJ, 107, 1786
VanderPlas, J. T., & Ivezic, Z. 2015, ApJ, 812, 18